Oil Shale, 2013, Vol. 30, No. 1, pp. 27–47 ISSN 0208-189X
doi: 10.3176/oil.2013.1.04

EFFECT OF HEATING RATE ON PRODUCTS YIELD AND CHARACTERISTICS OF NON-CONDENSABLE GASES AND SHALE OIL OBTAINED BY RETORTING DACHENGZI OIL SHALE

SHA WANG[(a)], JIAXUN LIU[(a)], XIUMIN JIANG[(a)*],
XIANGXIN HAN[(a)], JIANHUI TONG[(a,b)]

[(a)] Institute of Thermal Energy Engineering, School of Mechanical Engineering,
Shanghai Jiao Tong University, Shanghai 200240, P. R. China
[(b)] School of Materials Science and Engineering,
Jingdezhen Ceramic Institute, Jingdezhen 333001, P. R. China

Abstract. *Oil shale samples from Dachengzi mine located in Huadian city, Jilin province, China, were retorted in a stainless-steel cylindrical retort at a heating rate varied from 5 to 20* $^{o}C\ min^{-1}$ *up to a final temperature of 520* ^{o}C *under argon atmosphere. The influence of heating rate on the products yield and characteristics of shale oil and non-condensable gases was determined. It was observed that the shale oil yield first increased and then slightly diminished as the heating rate increased. The maximum shale oil yield was found to be 15.696 wt.% at a heating rate of 12* $^{o}C\ min^{-1}$*. The non-condensable gases yield increased with increasing heating rate. There was a corresponding decrease in the shale char yield. The carbon and nitrogen weight contents of the derived shale oil increased with increasing heating rate, while those of hydrogen and oxygen decreased. The sulfur weight content was not significantly affected by increasing the heating rate. As the heating rate increased from 5 to 20* $^{o}C\ min^{-1}$*, the atomic H/C and O/C ratios of the derived shale oil decreased from 1.918 to 1.727 and from 0.116 to 0.048, respectively. Compared to crude oils, the produced shale oil had a higher atomic O/C ratio and a similar atomic H/C ratio, as well as a higher light oil content, which showed that the properties of shale oil were superior to those of crude oil. The liquid shale oil could be classified as a sweet and high-nitrogen oil in terms of the classification method of crude oil. Increasing heating rate decreased the content of saturates and aromatics and increased that of light oil, asphaltenes and non-hydrocarbons of the produced shale oil. The non-condensable gases contained high amounts of* CH_4 *and minor concentrations of* C_2*-*C_4 *hydrocarbons. Increasing heating rate shifted the maximum concentration of* C_1*-*C_4 *hydrocarbons to higher temperature and increased the total content of* C_1*-*C_4 *hydrocarbons. The alkene/alkane gases*

---

[*] Corresponding author: e-mail *xiuminjiang@sjtu.edu.cn*

ratio decreased from 0.45 to 0.29 with increasing the heating rate from 5 to 20 °C min^{-1} which was linked to secondary reactions. The lower alkene/ alkane gases ratio was possibly because the coking reactions dominated at higher heating rate.

Keywords: *oil shale, retorting, heating rate, non-condensable gases, shale oil, yield, characteristics.*

1. Introduction

The world energy crisis and abrupt rises in the prices of oil derivatives have caused renewed interest in carbonaceous material as an energy source, such as coal, oil shale, biomass and organic wastes [1]. Oil shale, an organic-rich fine-grained sedimentary rock containing significant amounts of kerogen from which shale oil and synthetic gas can be produced through the chemical process of pyrolysis, represents a valuable potential source of liquid hydrocarbons and energy [2–6]. Currently, oil shale resources are widely distributed around the world and more than 600 deposits are known in more than 30 countries on all continents, with a conservatively estimated 4.8 trillion barrels of shale oil in place which is almost 4 times more than the proven crude oil resources of 1.3 trillion barrels [7, 8]. In China, it has been estimated that there is a vast and widespread oil shale resource across 22 provinces, 47 basins and 80 deposits with the total estimated in-place shale oil resource of about 48 billion tonnes [8, 9]. This huge reserve of energy sources in China is very significant for alleviating the pressure on petroleum supplies. For the energy potential of oil shale to be maximized, the conversion process of oil shale to shale oil should be undertaken under optimal process conditions. A range of process conditions have been investigated in the pyrolysis of oil shale to ensure the maximum and efficient extraction of oil. These parameters include pyrolysis temperature, pyrolysis atmosphere [10–14], heating rate [15–30], particle size [31, 32], mineral content [33], etc. Heating rate is one of the most important factors that exerts a significant influence on the reactions and products of the pyrolysis process.

Several investigators have studied the effect of heating rate on the total weight loss and products yield during the pyrolysis of oil shale. Most indicated that there is a shift in the maximum rate of weight loss to higher temperature with increasing heating rate [15–18]. However, there is some uncertainty in the literature regarding the influence of heating rate on the yield of non-condensable gases and shale oil. Campbell *et al.* [19] reported that the rate of methane release increased with decreasing heating rate varying from 0.5 to 4.0 °C min^{-1}. Nazzal [20], on the contrary, reported an increase in hydrocarbon gases content as the heating rate increased from 2 to 30 °C min^{-1}. On the other hand, Campbell *et al.* [21, 22] have indicated that more liquid oil was collected with increasing heating rate. Han *et al.* [23] also suggested that the heating rate lower than 10 °C min^{-1} had a significant positive effect on shale oil yield. However, the retorting process carried out at a heating rate higher than 10 °C min^{-1} may be a diffusion-limited process controlled by heat and product diffusion, resulting in the secondary reactions of shale oil and decreasing its yield [10, 20, 21]. Moreover, some authors indicated that little or no increase in oil yield was observed when the final retorting temperature was higher than 500 °C at a heating range of 4–55 °C min^{-1} [24]. At the same time, Al-Ayed *et al.* [25, 26] reported a decrease in oil yield and increase in shale oil density with increasing heating rate from 0.2 to 13 °C min^{-1} during pyrolysis of oil shale samples in a fixed-bed retort.

However, the effect of heating rate on the properties of non-condensable gases and shale oil produced by retorting oil shale has rarely been reported. The ratio of alkene to alkane gases in the evolved non-condensable gases has been used to determine reaction mechanisms and specify pyrolysis conditions. Campbell *et al.* [21] reported that ethene/ethane and propene/propane ratios increased with increasing heating rate in the range of 0.3–12 °C min^{-1}, which may result in the increase of vapor phase cracking [27, 28], while low alkene to alkane gases ratios at low heating rates may be related to secondary coking reactions [21]. Furthermore, it was concluded that the entire mechanism of oil shale pyrolysis and composition of the derived oil were heating rate dependent, the number of kerogen decomposition pathways being more diverse at higher heating rates [29]. Studying the properties of shale oil is considered an important step in the upgrading process and in evaluating the potential use of oil for different purposes, and assists in selecting and/or deciding appropriate technology requirements [30]. The shale oils produced at different heating rates have been investigated by elemental analysis and chemical class fractionation. Nazzal [20] put forward that the atomic H/C ratio decreased with increasing heating rate under both nitrogen and nitrogen/steam pyrolysis atmospheres. The decrease of the atomic H/C ratio indicated the production of oil more aromatic in nature and was also reflected by an increase in the density of the derived shale oil. In addition, the influence of heating rate on the aliphatics concentration in the derived oil was very small compared to that of aromatics. However, Al-Harahsheh *et al.* [30] demonstrated that the hydrogen and sulfur contents of the produced shale oil increased with increasing carbon weight percent while the H/C was not affected in the heating rate range of 0.2–6 °C min^{-1} studied. Additionally, the researchers showed that with increasing heating rate the content of aliphatics of the liquid shale oil increased and that of the aromatic fraction decreased.

In this paper, oil shale samples from Dachengzi mine located in Huadian city of China were retorted in a stainless-steel cylindrical retort at different heating rates in order to determine the dependence of products yield and properties of shale oil and non-condensable gases on heating rate. The shale oil produced was subjected to elemental analysis, high temperature simulated distillation and SANA (saturates, aromatics, non-hydrocarbons, and asphaltenes) fractionation. Additionally, the hydrocarbon gases (C_1-C_4)

composition in the non-condensable gases has been analyzed. Such information is needed not only to understand the process reaction mechanisms, but also to optimize the process and enhance shale oil yield and quality.

2. Experimental

2.1. Shale sample

The oil shale samples investigated in this paper were obtained from Dachengzi mine located in Huadian city, China. Table 1 shows the general characteristics of the samples. The original oil shale samples were sampled, crushed, ground and sieved to a grain size of 0–3 mm, considering the National Standards of China (GB 474-1996). All samples were dried in an oven at 105 °C for a period of 10–12 h, and then stored in a desiccator avoiding any adsorption of water or loss of volatiles.

Table 1. Proximate and ultimate analysis of Dachengzi oil shale

Proximate analysis, ar		Ultimate analysis, wt.%, ar	
Moisture, wt.%	11.54	C	27.33
Volatile matter, wt.%	36.21	H	3.59
Ash, wt.%	48.24	O	7.89
Fixed carbon, wt.%	4.01	N	0.57
Low heating value, kJ/kg	11076.07	S	0.84

2.2. Retorting system

All experiments were conducted in a stainless-steel cylindrical retort (70 mm i.d., 100 mm height). 50 g of dried oil shale samples were placed inside the retort before each test and electrically heated from room temperature to a final retorting temperature of 520 °C at a rate of 5, 8.5, 12 and 20 °C min^{-1} and held at 520 °C for 20 min using argon as the purge gas. The oven temperature controlled and monitored by a digital temperature controller was indicated by an oven thermocouple (Fig. 1), which was situated between the external body of the retort and the inner side of the ceramic cylinder. Heating rate was controlled through changing the power supply voltage input to the retort heater. The argon sweep gas at a rate of 0.3 L min^{-1} was introduced from the top of the retort in an 8 mm pipe for preheating while passing downward to the bottom of the retort and was then allowed to disperse to sweep the generated products toward the retort side outlet to minimize secondary reactions [10]. The liquid products were trapped in a series of cold traps which were immerged in low-temperature troughs (~0 °C) filled with the mixture of ice and water, while the non-condensable gases were directed through the U-tube and mixed with argon at a rate of 2.7 L min^{-1}. Part of the gas mixture was sampled into the online gas analyzer for analyzing the component concentrations as a function of time and then vented from the gas analyzer outlet into the atmosphere. The other gas mixture also was also vented into the atmosphere via a flowmeter which kept the volume flow of gases into the analyzer constant (3 L min^{-1}). After the retorting temperature was held for a specified residence time, the experiment ceased. Shale char and the mixture of shale oil and water were collected and weighted, respectively. The non-condensable gases yield was determined by overall material balance. The derived oil consisted of an aqueous phase and oil phase. The oil was separated from the aqueous phase by centrifuging, decanting and removing the aqueous phase by a pipette for specific analysis [20, 34, 35]. In order to assess the reproducibility, each retorting test was performed twice under identical conditions.

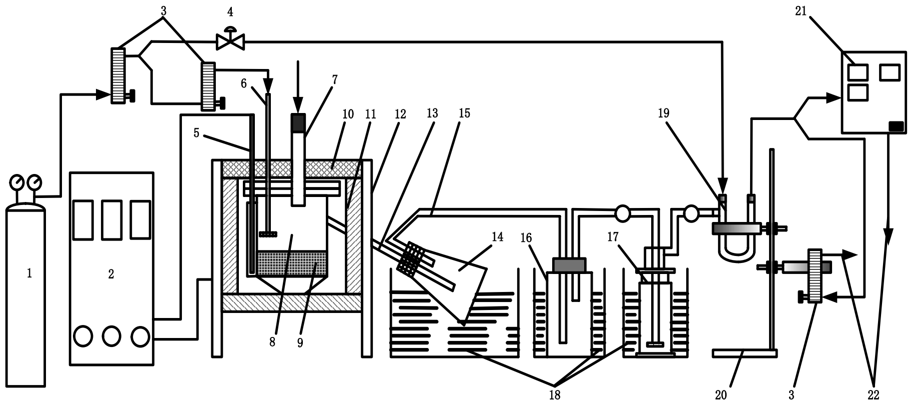

Fig. 1. Schematic diagram of the experimental oil shale retorting system. 1 – argon cylinder, 2 – automatic temperature controller, 3 – flowmeter, 4 – flow control valve, 5 – thermocouple, 6 – gas inlet, 7 – sample inlet, 8 – retort reactor, 9 – oil shale, 10 – insulation, 11 – electric heater, 12 – steel stand, 13 – copper tube, 14 – conical flask, 15 – silicone tube, 16 – widemouthed bottle, 17 – gas washing bottle, 18 – water/ice condenser, 19 – U-tube, 20 – stand, 21 – gas analyzer, 22 – vent.

2.3. Gas analysis

The gas mixture sample emitted from the U-tube was continuously led to an on-line Fourier transform infrared (FTIR) gas analyzer (Gasmet DX-4000, Gasmet Technologies, USA; 8 cm^{-1} resolution, high path gas cell of a length of 9.8 m). The gas analyzer was composed of two units: the sampling unit for gases sampling and cleaning, and the measuring unit for continuous analysis with an FTIR analyzer. Before every test, the background spectrum was recorded when argon flowed through the sample cell at a rate of 1.2 L min^{-1}. Then the sample was continuously measured by the analyzer at 1.046 bar and 180 ^{o}C, and the sample spectra were recorded. The infrared spectra obtained were processed by Calcmet Software 2005 which was connected to the analyzer via RS232. The FTIR spectra were recorded for the following components: NO, NO_2, N_2O, NH_3, CH_4, C_2H_6, C_3H_8, C_4H_{10}, C_2H_4, C_3H_6, C_4H_8, C_2H_2, SO_2, CS_2, CO, CO_2, and H_2O. This paper mainly investigated C_1-C_4 hydrocarbon gases.

2.4. Oil analysis

2.4.1. Elemental analysis

The shale oil samples were analyzed for CHNO using a Vario EL cube CHNOS elemental analyzer (Elementar, Germany), and for the total sulfur content by a Jena EA3100 NS analyzer (Carl Zeiss, Germany).

2.4.2. High temperature simulated distillation

The boiling point distribution of liquid products was obtained by high temperature simulated distillation (HTSD) using an ASTM method HT 750 (AC Analytical Controls Method; Analytical Controls, Inc., USA). This HTSD analysis was performed with an Agilent 6890N gas chromatograph (Agilent Technologies, Inc., USA) which was equipped with an autosampler and an automatic injector. The carrier gas was helium (99.999% purity) with a constant flow rate of 3 mL min^{-1}. The GC contained a 5 m × 0.53 µm × 0.09 µm capillary column (AC SIMDIS HT 750; Analytical Controls, Inc., USA) with a cool on-column injector. Temperature programming for the column was 10 ^{o}C min^{-1} from 40 to 430 ^{o}C (maintained for 5 min). The on-column injector was programmed from 100 to 430 ^{o}C (run time 22 min) with a temperature gradient of 15 ^{o}C min^{-1}. The flame ionization detector (FID) was maintained at 430 ^{o}C.

2.4.3. Separation of different fractions from shale oil

The SANA (saturates, aromatics, non-hydrocarbons, and asphaltenes) fractionation of shale oil samples was carried out using the Chinese Petroleum Industrial Standard SY/T 5119-2008. A total of 30 mL of hexane was added to 50 mL of shale oil sample. The mixture sat for 12 h and was then filtered through a funnel covered with cotton wool. The hexane-insoluble matter on the cotton wool was washed with hexane until the filtrate was clear. The hexane-insoluble asphaltenes remaining on the cotton wool were dissolved and washed by dichloromethane. The hexane-soluble matter collected was subjected to saturate, aromatic, and non-hydrocarbon fractionation. A glass column (8 mm i.d. × 300 mm length) was packed with 3 g of silica gel (80–100 mesh, activated at 150 ^{o}C for 8 h) and 2 g of neutral alumina (100–200 mesh, activated at 400 ^{o}C for 4 h). Cotton wool was inserted at the bottom of the column. After the hexane-soluble matter was poured through the packed column, 25 mL of hexane was added to elute the saturate fraction. The aromatic fraction was obtained by eluting the column with a 15 mL mixture of hexane/dichloromethane (1:1, v/v). The non-hydrocarbon fraction was obtained by eluting the column with 10 mL of ethanol, followed by 15 mL of chloroform.

3. Results and discussion

3.1. Products yield

Figure 2 shows the yield of shale oil, water, non-condensable gases and shale char as a function of heating rate. It is clear that increasing the heating rate from 5 to 12 °C min^{-1} causes an increase in the shale oil yield from 14.441 to 15.696 wt.%. A further increase of the heating rate leads to a slight decrease in the shale oil yield. These results agree with those reported by Nazzal [20] for a heating rate range of 2–30 °C min^{-1}. Nazzal [20] indicated that the permeability of oil shale is insufficient to allow an external sweep gas to significantly penetrate a shale block. The self-generated intraparticle gas sweep and oil vaporization processes are the only effective means to remove oil from the shale block. At lower heating rates, the shale oil products generated from oil shale diffuse out of the sample under a slower internal autogeneous gas sweep rate and remain within a given temperature range for a longer period of time. This may allow secondary reactions resulting in the increase of coke formation and decrease of oil yield. In addition, secondary gas phase cracking reactions may also result, but to a lesser extent, because the oil evolved from the particle is at lower temperatures [10]. Additionally, the higher heating rate might allow the recovery of more oil because it generated higher self-generated gas sweep rates during retorting. Campbell *et al.* [21] also suggested that the heating rate of 0.2–3 °C min^{-1} should not affect oil yield, but should control some other degradation mechanisms of oil before being collected. They considered that coking was the major intraparticle oil degradation process which was reduced by increasing the heating rate up to 9 °C min^{-1}. Furthermore, Nazzal [20] indicated that the oil removed from the oil shale particle could be coked on the spent shale. The

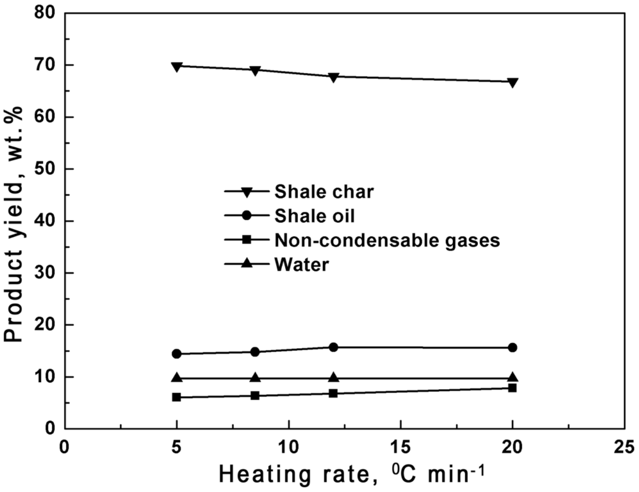

Fig. 2. Effect of heating rate on the yield of products derived by retorting Dachengzi oil shale.

coking losses were possibly reduced by choosing a sweep gas which might be adsorbed on the shale particles and block the access of oil molecules by a cheap gas, such as CO_2, N_2, or steam.

In this paper, increasing the heating rate from 12 to 20 $^{o}C\ min^{-1}$ causes a slight decrease of 0.078 wt.% in shale oil yield, as shown in Fig. 2. These results agree with those obtained by Han *et al.* [23] and this slight decrease in the liquid yield may be attributed to the fact that the heating rate has a little effect on the self-generated gas sweep retorting. Williams and Ahmed [10] suggested that the pyrolysis process at a heating rate higher than 10 $^{o}C\ min^{-1}$ may be a diffusion-limited process controlled by heat and product diffusion. They considered that the extent of diffusion control increases at high heating rates because products are generated faster than they can diffuse out of the pores, consequently, secondary coking reactions will occur. The extent of diffusion control diminishes during the reaction as the shale changes from impervious rock to porous ash as the pyrolysis products leave the matrix [23]. Nazzal [20] also put forward that at higher heating rates, the pyrolysis vapors are produced at a higher rate than they can escape from the pores in which they are located as porosity has insufficient time to develop, consequently, oil coking will occur and oil yield diminish. Also, because the oil diffusing out of the particle will meet higher temperatures, gas phase cracking reactions will increase, resulting in a decrease of oil yield. Therefore, an optimum heating rate of about 12 $^{o}C\ min^{-1}$ is recommended for the sample and reactor conditions in this work.

On the other hand, Fig. 2 also shows that there is an increase in the evolved non-condensable gases yield by increasing the heating rate from 5 to 20 $^{o}C\ min^{-1}$. The water content is found to be 9.7 ± 0.02 wt.%. The heating rate has a little effect on the shale char yield, which decreases from 69.82 to 66.828 wt.% as the heating rate increases from 5 to 20 $^{o}C\ min^{-1}$.

3.2. Oil analysis

3.2.1. Elemental analysis (CHN)

Table 2 presents the elemental analysis of carbon, hydrogen, nitrogen, oxygen and sulphur and the atomic H/C and O/C ratios of the derived oil as a function of heating rate varying from 5 to 20 $^{o}C\ min^{-1}$. The carbon content of oil increases from 74.32 to 78.21 wt.% and that of hydrogen decreases from 11.88 to 11.32 wt.%. In addition, the nitrogen content increases from 0.88 to 1.05 wt.% with increasing heating rate because the nitrogen in the shale char or non-condensable gases may participate in the aromatization process to form polycyclic aromatic nitrogen hydrocarbons (PNAHs). But increasing heating rate causes the oxygen content to obviously decrease from 11.54 to 4.98 wt.%, which is mainly because more oxygen transforms to non-condensable gases or shale char. Additionally, it is worth noting that the sulfur weight percent of liquid shale oil is not significantly affected by the increasing heating rate due to its entanglement with metal oxides and the nature of chemical bonding with hydrocarbons. This result agrees with the finding reported by Al-Harahsheh *et al.* [30]. The carbon and hydrogen contents in the derived shale oil are slightly lower than those in crude oils (Table 3). However, nitrogen, oxygen and sulfur contents are higher.

Table 2. Elemental analysis of the shale oil derived by retorting Dachengzi oil shale as a function of heating rate, wt.% of oil

Element	Heating rate, °C min^{-1}			
	5	8.5	12	20
Carbon	74.32	77.19	77.59	78.21
Hydrogen	11.88	11.6	11.46	11.32
Nitrogen	0.88	0.97	0.99	1.05
Oxygen	11.54	10.13	5.55	4.98
Sulfur[a]	0.38	0.37	0.39	0.38
The sum of carbon and hydrogen	86.2	88.79	87.05	89.53
Atomic (H/C) ratio	1.918	1.803	1.772	1.727
Atomic (O/C) ratio	0.116	0.098	0.054	0.048

[a] The total content of sulfur was determined with a Jena EA3100 NS analyzer.

Table 3. Elemental analysis of crude oils of China, wt.% of oil

Element	Oil samples		
	Daqing[c]	Shengli[d]	Xinjiang[e]
Carbon	85.87	86.26	86.13
Hydrogen	13.73	12.2	13.3
Nitrogen	0.16	0.41	0.13
Oxygen[b]	0.14	0.33	0.39
Sulfur	0.1	0.8	0.05
The sum of carbon and hydrogen	99.6	98.46	99.43
Atomic (H/C) ratio	1.9	1.68	1.84
Atomic (O/C) ratio	0.0012	0.0029	0.0034

[b] By difference.

[c] Daqing crude oil is obtained from Daqing oil field located in Heilongjiang province, China.

[d] Shengli crude oil is obtained from Shengli oil field located in Shandong province, China.

[e] Xinjiang crude oil is obtained from Xinjiang oil field located in Xinjiang Uygur Autonomous Region, China.

Additionally, Table 2 shows that the atomic O/C and H/C ratios decrease from 0.116 to 0.048 and from 1.918 to 1.727, respectively, by increasing the heating rate from 5 to 20 °C min^{-1}. The atomic O/C ratio is obviously higher than that of crude oils, while the atomic H/C ratio is close to that of crude oils. This decrease of the atomic H/C ratio may indicate the production of oil more aromatic in nature. Burnham [36] proposed that the increase of the nitrogen content and the decrease of the atomic H/C ratio of oil may be due to that the nitrogen in the oil is contained in aromatic molecules which are resistant to cracking and are thermodynamically more stable. In addition, Stout *et al.* [37] reported that the oil properties changed with oil yield and the H/C ratio increased as the oil yield decreased. They suggested that the yield loss caused by coking reactions increased the hydrocarbon content in the derived oil because of the condensation and polymerization reactions involving nitrogen-containing gas compounds. This agrees with the results obtained in this work at a heating rate lower than 12 °C min^{-1}.

Moreover, the shale oil produced by retorting Dachengzi oil shale is classified as a sweet and high-nitrogen crude oil in terms of the classification method of crude oil (Table 4) [38].

Table 4. Classification of crude oil based on sulfur and nitrogen contents, wt.% of oil

Type of crude oil	S	Type of crude oil	N
Sweet crude oil	<0.5	Low-nitrogen crude oil	<0.25
Sour crude oil	0.5–2	High-nitrogen crude oil	>0.25
High-sulfur crude oil	>2		

3.2.2. High temperature simulated distillation

Figure 3 shows the effect of heating rate on the simulated distillation of the shale oil derived from Dachengzi oil shale by retorting. The initial boiling point (IBP) of the shale oil retorting at 5, 8.5, 12 and 20 °C min^{-1} is 72.2, 58.6, 58.6 and 52.6 °C, respectively. But all shale oil samples have the same final boiling point (FBP) of 750 °C. The plot indicates that increasing the heating rate causes the increase of the lighter fraction in the shale oil.

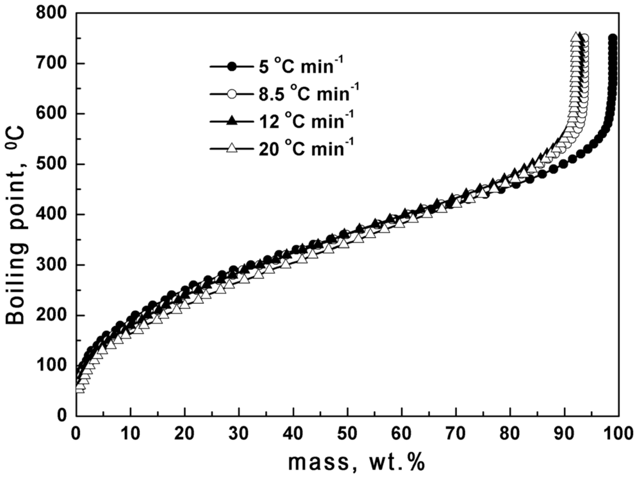

Fig. 3. Effect of heating rate on the simulated distillation of the shale oil derived by retorting Dachengzi oil shale.

Furthermore, Table 5 also suggests that the produced shale oils have fractions with a wide range of boiling points, mainly a 10.9–16.1 wt.% light naphtha fraction (IBP ~200 °C), 34.1–36 wt.% medium fractions, which can be used as diesel oil (200–350 °C), and 48–53.1 wt.% heavy fractions (>350 °C). The light naphtha fraction (IBP ~200 °C) increases from 10.9 to 16.1 wt.% by increasing the heating rate from 5 to 20 °C min^{-1}. It is concluded that the secondary reactions of oil result in not only a low oil yield but also a highly valuable light naphtha fraction.

Figure 4 shows the distillate fractions at intervals of 30 °C of the shale oil produced at different heating rates. The light naphtha fraction (IBP ~200 °C) and the medium fraction (200–350 °C) have a normal distribution, with mean values of 110 and 240 °C, respectively. This distribution favors the cut of the

Table 5. Distillate fractions of the shale oil derived by retorting Dachengzi oil shale and crude oils produced in China, wt.% of oil

Oil fraction	Heating rate	Light fraction (IBP~200 °C)	Medium fraction (200–350 °C)	Heavy fraction (>350 °C)
Shale oil	5 °C min^{-1}	10.9	36	53.1
	8.5 °C min^{-1}	12.8	34.7	52.5
	12 °C min^{-1}	13.1	34.1	52.8
	20 °C min^{-1}	16.1	35.9	48
Crude oils produced in China	Daqing	11.5	19.7	68.8
	Shengli	7.6	17.5	74.9
	Xinjiang	15.4	26	59.6

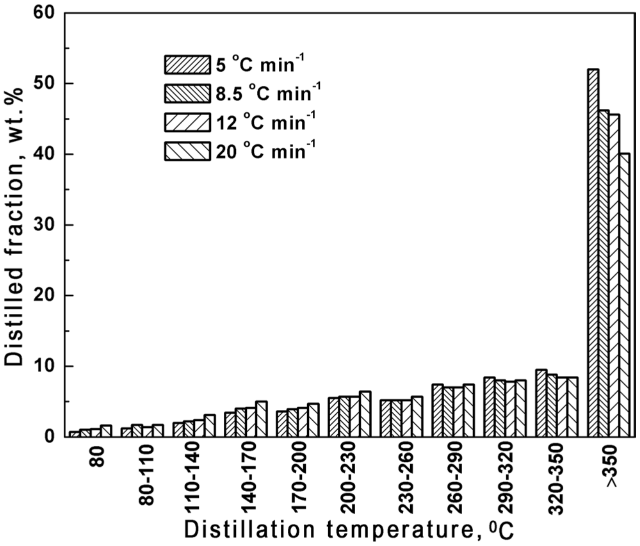

Fig. 4. Effect of heating rate on distillate fractions in the shale oil derived by retorting Dachengzi oil shale.

shale oil as the naphtha and diesel oil in potential applications. In addition, Table 5 also compares the distillate fractions of the shale oil and three crude oils of China (Daqing of Heilongijang province, Shengli of Shandong province, and Xinjiang of Uygur Autonomous Region) [39]. The crude oil has a 59.6–74.9 wt.% heavy fraction (>350 °C), while the shale oil only contains a 48–53.1 wt.% heavy fraction. The shale oil is much lighter than crude oil. Therefore, it is considered that the properties of shale oil are superior to those of crude oil.

3.2.3. SANA fractions

Figure 5 shows the weight percent of SANA fractions of the derived shale oil as a function of heating rate. From the available data it can be seen that increasing the heating rate from 5 to 12 °C min^{-1} causes the content of asphaltenes and non-hydrocarbons slightly to increase. A further increase of the heating rate results in an appreciable increase in the asphaltenes yield. It is also clear that increasing the heating rate decreases the content of saturate and aromatic fractions. The decrease of the saturate fraction is about twice that of the aromatic fraction. The saturates content in the shale oil derived is close to 60 wt.%. On the one hand, this can be explained by the kerogen decomposition mechanism. Williams [40] suggested that kerogen pyrolysis occurs in two main steps. First, the insoluble kerogen breaks down into benzene soluble bitumen, and then the bitumen cracks thermally into oil, water and gases. In addition, Wallman *et al.* [41] proposed a reaction network of oil shale pyrolysis. Kerogen is thermally decomposed to light oil, bitumen, and water vapor. This rate of decomposition is reasonably fast and is of the order of one minute at 500 °C. The physical nature of the bitumen

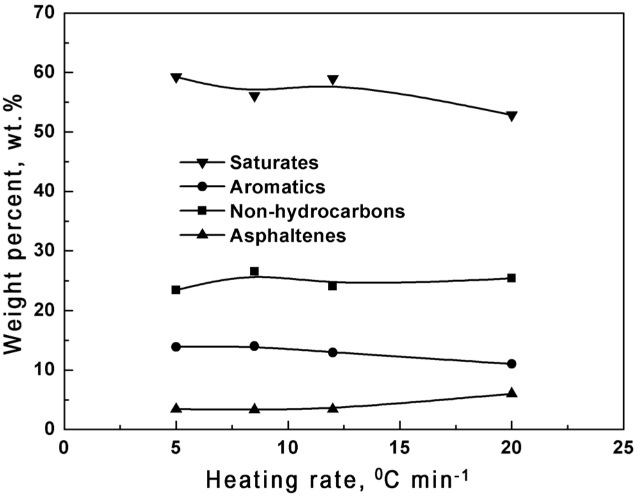

Fig. 5. Weight percent of SANA fractions of the shale oil derived by retorting Dachengzi oil shale as a function of heating rate.

formed in this reaction is not fully understood. Presumably, it is in the plastic state and the diffusion of bitumen in such a state is assumed negligible. This bitumen undergoes two further parallel reactions. In one reaction, heavy oil is produced. The rate of this heavy oil production is far slower than that of kerogen thermal decomposition, and is of the order of 15 minutes at 500 °C. In the other reaction, gases and coke are formed at the ratio of 1:4 established by Wallman *et al.* [41]. The light oil and heavy oil are further cracked to give gases and light oil, respectively. In this work, as the heating rate increases, the oil shale sample is heated faster in a short period of time and kerogen is decomposed to light oil, bitumen, and water vapor faster. The bitumen is generated faster than it further decomposes because it remains within a given temperature range for a shorter period of time at a higher heating rate. As a result, the content of the light oil produced from kerogen in the first reaction step increases and the content of the heavy oil and light oil produced from bitumen in the second reaction step decreases with increasing heating rate. This result is consistent with data presented in Table 5. In addition, the amount of unreacted bitumen increases as the heating rate increases, so there is an increase in the asphaltenes content and decrease in that of aromatics and saturates. This is mainly because bitumen is a complex mixture of organic and inorganic compounds which may be separated into asphaltenes and maltenes. Asphaltenes constitute a complex mixture of heavy hydrocarbons and heteroatom- and metal-containing hydrocarbon oligomers which are insoluble in aliphatic hydrocarbon solvents (n-pentane and n-heptane). Maltenes are composed of saturate compounds, aromatic compounds and non-hydrocarbons which are soluble in n-heptane [42, 43]. The higher the heating rate is, the less asphaltenes and maltenes decompose to gases, oil and coke in the second reaction step.

On the other hand, at low heating rates, the oil loss is mainly due to secondary coking reactions when oil products diffuse out of the sample at a low internal autogeneous gas sweep rate [10, 20, 21]. Additionally, there are possibly also secondary gas phase cracking reactions resulting in oil loss. In this paper it was found that as the heating rate increases, secondary gas phase cracking and oil coking reactions may occur. The gas-phase cracking of aliphatics (free and those attached to aromatics) or Diels–Alder type reactions may result in the formation of aromatics by the selective concentration of aromatic compounds [20, 36]. But the coking reactions of aromatics dominate at higher heating rate because the increasing production of asphaltenes, as coke precursors, is responsible for the coke deposition. So, the saturates and aromatics contents decrease with increasing heating rate, and the influence of heating rate on the saturates content is more significant.

3.3. Analysis of non-condensable gases

Figure 6 shows the effect of heating rate on the volume percent of hydrocarbon gases (alkanes (C_1-C_4) and alkenes (C_2-C_4)) as a function of retorting temperature. As the heating rate increases, the maximum concentration of

(a) CH_4

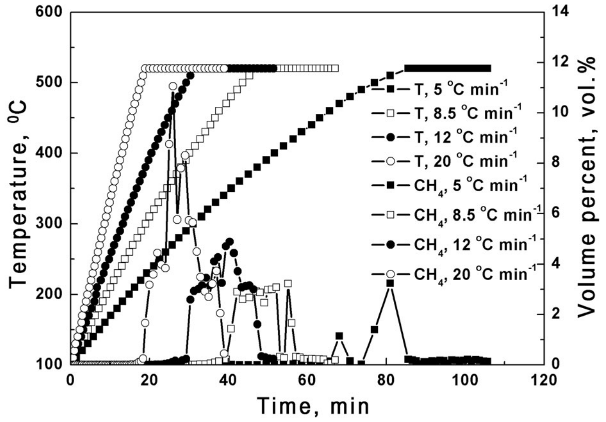

(b) C_2H_6

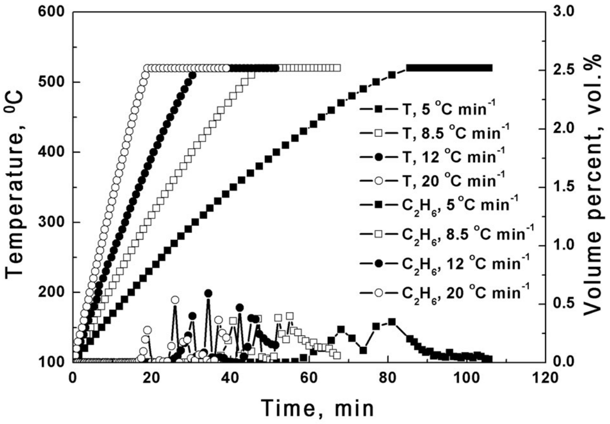

(c) C_2H_4

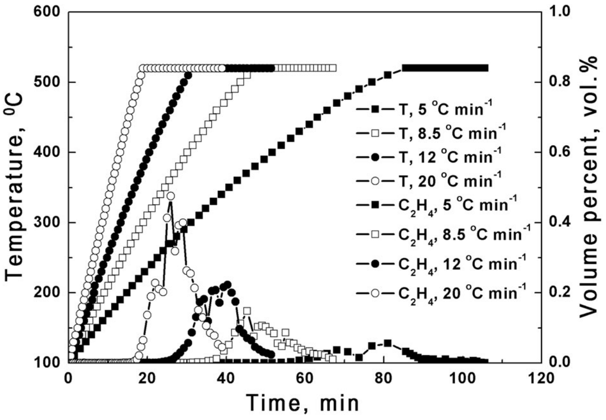

Fig. 6. Effect of heating rate on the volume percent of hydrocarbon gases as a function of retorting temperature.

(d) C_3H_8

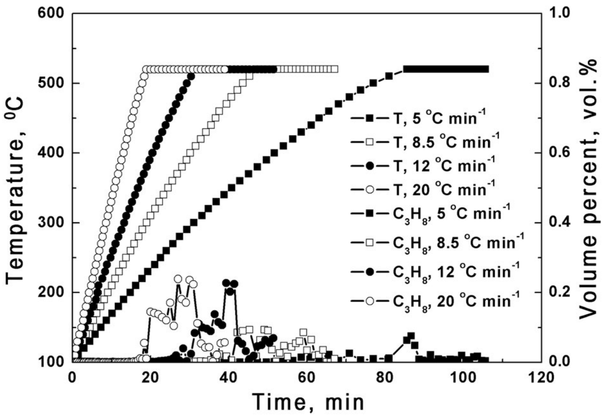

(e) C_3H_6

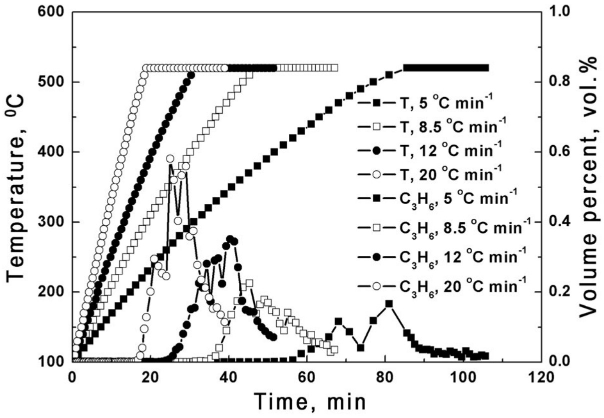

(f) C_4H_{10}

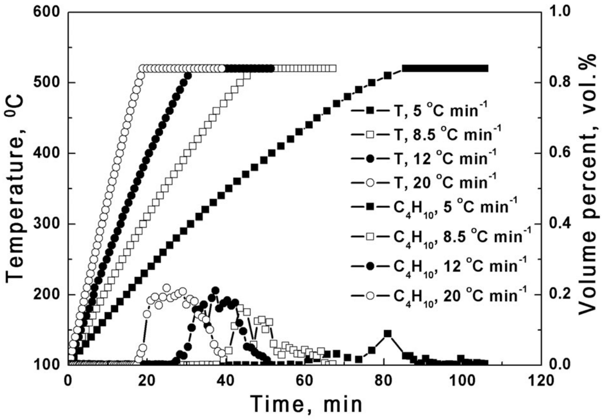

Fig. 6 (continuation).

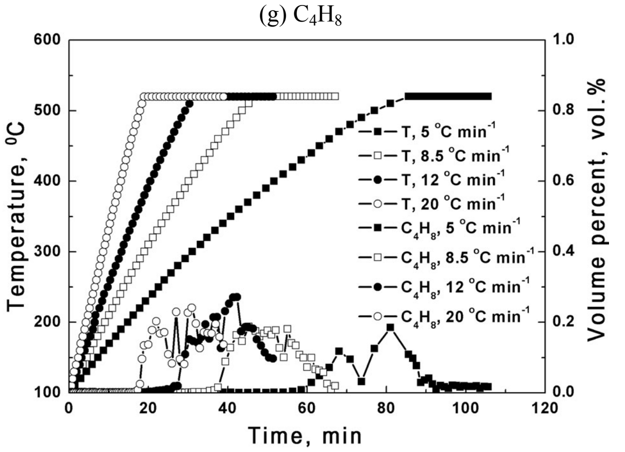
(g) C_4H_8

Fig. 6 (continuation).

most gases occurs at higher temperature and increases. At the heating rate of 5 °C min^{-1}, the methane formation and evolution begin at a temperature slightly lower than 350 °C and reach a maximum value at 480 °C. The C_2 (ethane and ethene) production increases to a maximum value at 470 °C as does that of C_3 (propane and propene). There is a large amount of CH_4, which is significantly affected by the heating rate, but small concentrations of C_2-C_4 in the non-condensable gases. This is also demonstrated in Table 6 which suggests that increasing the heating rate causes the increase of C_1-C_4. These results indicate that significant secondary reactions may occur, which increases the formation of hydrocarbon gases and decreases the shale oil yield. This result agrees with that observed by Williams and Ahmed [10] and Campbell *et al.* [21, 22]. The decrease of saturates and aromatics concentrations in the derived oil at higher heating rate supports these findings.

Table 6 also presents the ethene/ethane, propene/propane, butene/butane and total alkene/alkane ratios. The ratio of alkene to alkane gases in the evolved pyrolysis gases has been used to determine reaction mechanisms and specify pyrolysis conditions [27, 28]. Raley [27] has suggested a mechanism to explain the correlation between the alkene/alkane ratio and heating rate as a free radicals chain reaction scheme. The dependence of the alkene/alkane ratio on heating rate is attributed to the competition between carbon–carbon bond cleavages versus hydrogen atmosphere processes. He associated the increased ethene/ethane and propene/propane ratios with the increased vapour phase cracking and decreased oil yield. Campbell *et al.* [21] reported that the ethene/ethane, propene/propane and alkene/alkane ratios increased with increasing heating rate in a range of 0.3–12 °C min^{-1}. This is linked to secondary gas phase reactions [28].

Table 6 shows that there are no conclusive trends in ethene/ethane, propene/propane and butene/butane ratios as a function of heating rate, while the alkene/alkane ratio decreases with increasing heating rate. The high alkene/alkane ratios at low heating rates are possibly linked to secondary gas phase cracking reactions. Similarly, at high heating rates both coking reactions, which tend to reduce the alkene/alkane ratio, and cracking reactions, which increase this ratio, may take place [10]. The lower alkene/alkane ratio is possibly because the coking reactions dominate at higher heating rate.

Table 6. Composition of hydrocarbon gases derived by retorting Dachengzi oil shale as a function of heating rate, mg/Nm^3

Hydrocarbon gases	Heating rate, ^{o}C min^{-1}			
	5	8.5	12	20
Methane	1850.85	4438.26	8843.57	17715.48
Ethane	917.88	1001.83	1113.54	1476.28
Propane	148.36	395.05	789.64	1217.21
Butane	276.01	714.29	1306.95	2090.59
Ethene	125.80	348.82	668.13	1420.77
Propene	546.49	988.68	1698.84	2985.97
Butene	756.97	1322.44	2005.66	2158.46
Total alkanes (C_1-C_4)	3193.10	6549.44	12053.70	22499.56
Total alkenes	1429.26	2659.94	4372.64	6565.19
Total hydrocarbon gases	4622.37	9209.37	16426.34	29064.76
Ethene/ethane	0.14	0.35	0.60	0.96
Propene/propane	3.68	2.50	2.15	2.45
Butene/butane	2.74	1.85	1.53	1.03
Alkenes/alkanes	0.45	0.41	0.36	0.29

4. Conclusions

The overall experimental results show that heating rate has a significant influence on the products yield and characteristics of shale oil and non-condensable gases. The following conclusions can be inferred:

(1) As the heating rate increases from 5 to 20 ^{o}C min^{-1}, the shale oil yield increases and then slightly decreases, and the amount of evolved non-condensable gases slightly increases while that of shale char somewhat decreases. The heating rate has a low effect on water yield. This increase in shale oil yield has been attributed to the higher self-generated gas sweep rates generated at high heating rates (but still lower than 12 ^{o}C min^{-1}), reducing the degree of oil decomposition. The lower heating rate maintains the material within a given temperature range for a longer period of time, increasing the degree of oil decomposition.

(2) Increasing the heating rate from 5 to 20 ^{o}C min^{-1} increases the carbon and nitrogen content, while decreases that of hydrogen and oxygen, and the atomic H/C ratio in the derived shale oil. This decrease of the atomic H/C ratio indicated the production of oil more aromatic in nature and was also

reflected by an increase in the density of the derived shale oil. The increase of the nitrogen content and the decrease of that of oxygen are due to that the nitrogen in the shale char or non-condensable gases may participate in the aromatization process to form polycyclic aromatic nitrogen hydrocarbons (PNAHs) and more oxygen transforms to non-condensable gases or shale char. The sulfur content is not significantly affected by increasing heating rate due to its entanglement with metal oxides and the nature of chemical bonding with hydrocarbons.

(3) The carbon and hydrogen contents in the derived shale oil are slightly lower than those in crude oils, while nitrogen, oxygen and sulfur contents are higher. The produced shale oil has obviously a higher atomic O/C ratio and a similar atomic H/C ratio compared to crude oils. The shale oil derived from Dachengzi oil shale by retorting is characterized as a sweet and high-nitrogen crude oil in terms of the classification method of crude oil.

(4) Increasing the heating rate causes the increase of the lighter fraction in the shale oil. It is concluded that the significant secondary reactions of oil result in not only a low oil yield but also a highly valuable light naphtha fraction. The light naphtha fraction (IBP ~200 ^{o}C) and the medium fraction (200–350 ^{o}C) have a normal distribution, with mean values of 110 and 240 ^{o}C, respectively. This distribution favors the cut of shale oil as the naphtha and diesel oil in potential applications. The shale oil is much lighter than crude oil, which indicates that the properties of shale oil are superior to those of crude oil.

(5) Increasing the heating rate from 5 to 12 ^{o}C min^{-1} causes the asphaltenes and non-hydrocarbons contents to slightly increase. A further increase of the heating rate causes an appreciable increase in the asphaltenes yield. But increasing the heating rate decreases the content of saturate and aromatic fractions. The decrease of the saturate fraction is about twice that of the aromatic fraction. This can be explained by the kerogen decomposition mechanism and secondary reactions. The coking reactions of aromatics dominate at higher heating rate because the increasing production of asphaltenes, as coke precursors, is responsible for the coke deposition.

(6) As the heating rate increases from 5 to 20 ^{o}C min^{-1}, the maximum concentration of most hydrocarbon gases occurs at higher temperature and increases. At the heating rate of 5 ^{o}C min^{-1}, the contents of C_2-C_4 hydrocarbon gases reach a maximum value at 470 ^{o}C while that of methane reaches a maximum value at 480 ^{o}C. There is a high amount of CH_4 which is significantly affected by the heating rate, and small concentrations of C_2-C_4 in the non-condensable gases. Increasing the heating rate causes the increase of C_1-C_4.

(7). There are no conclusive trends in ethene/ethane, propene/propane and butene/butane ratios as a function of heating rate, while the alkene/alkane ratio decreases with increasing heating rate. The high alkene/alkane ratios at low heating rates are possibly linked to secondary gas phase cracking reactions. Similarly, at high heating rates both coking reactions, which tend to reduce the alkene/alkane ratio, and cracking reactions, which increase this ratio, may take place. The lower alkene/alkane ratio is possibly because the coking reactions dominate at higher heating rate.

Acknowledgement

The authors wish to express their gratitude to the State Key Laboratory of Heavy Oil Processing of China University of Petroleum for shale oil samples analysis and technical advice. This work was supported by the National Natural Science Foundation of China (Grant No. 50906051).

REFERENCES

1. Yanik, J., Seçim, P., Karakaya, S., Tiikma, L., Luik, H., Krasulina, J., Raik, P., Palu, V. Low-temperature pyrolysis and co-pyrolysis of Göynük oil shale and terebinth berries (Turkey) in an autoclave. *Oil Shale*, 2011, **28**(4), 469–486.
2. Dyni, J. R. Geology and resources of some world oil-shale deposits. *Oil Shale*, 2003, **20**(3), 193–252.
3. Altun, N. E., Hiçyilmaz, C., Hwang, J.-Y., Bağci, A. S., Kök, M. V. Oil shales in the world and Turkey; reserves, current situation and future prospects: a review. *Oil Shale*, 2006, **23**(3), 211–227.
4. Qian, J. L., Wang, J. Q., Li, S. Y. Oil shale development in China. *Oil Shale*, 2003, **20**(3S), 356–359.
5. Kök M. V. Evaluation of Turkish oil shales – thermal analysis approach. *Oil Shale*, 2001, **18**(2), 131–138.
6. Kök, M. V. Thermal investigation of Seyitomer oil shale. *Thermochim. Acta*, 2001, **369**(1–2), 149–155.
7. Liive, S. Oil shale energetics in Estonia. *Oil Shale*, 2007, **24**(1), 1–4.
8. Dyni, J. R. Oil shale. In *2010 Survey of Energy Resources* (Clarke, A. W., Trinnaman, J. A., eds.). World Energy Council, 2010, 93–123. http:// www.worldenergy.org/ documents/ser_2010_report_1.pdf.
9. Dyni, J. R. Oil shale. In *2007 Survey of Energy Resources* (Clarke, A. W., Trinnaman, J. A., eds.). World Energy Council, 2007, 93–123. http:// www.worldenergy.org/documents/ser2007_final_online_version_1.pdf.
10. Williams, P. T., Ahmad, N. Influence of process conditions on the pyrolysis of Pakistani oil shales, *Fuel*, 1999, **78**(6), 653–662.
11. Dung, N. V. Factors affecting product yields and oil quality during retorting of Stuart oil shale with recycled shale: a screening study. *Fuel*, 1995, **74**(4), 623–627.
12. El harfi, K., Mokhlisse, A., Ben Chanâa, M. Yields and composition of oil obtained by isothermal pyrolysis of the Moroccan (Tarfaya) oil shales with steam or nitrogen as carrier gas. *J. Anal. Appl. Pyrol.*, 2000, **56**(2), 207–218.
13. Kök, M. V., Pamir, M. R. Non-isothermal pyrolysis and kinetics of oil shales. *J. Therm. Anal. Calorim.*, 1999, **56**(2), 953–958.

14. Kök, M. V., Senguler, I., Hufnagel, H., Sonel, N. Thermal and geochemical investigation of Seyitomer oil shale. *Thermochim. Acta*, 2001, **371**(1–2), 111–119.
15. Kök, M. V. Heating rate effect on the DSC kinetics of oil shales. *J. Therm. Anal. Calorim*., 2007, **90**(3), 817–821.
16. Kök, M. V., Pamir, R. Pyrolysis kinetics of oil shales determined by DSC and TG/DTG. *Oil Shale*, 2003, **20**(1), 57–68.
17. Olivella, M. A., De Las Heras, F. X. C. Evaluation of linear kinetic methods from pyrolysis data of Spanish oil shales and coals. *Oil Shale*, 2008, **25**(2), 227–245.
18. Wang, Q., Sun, B. Z., Hu, A. J., Bai, J. R., Li, S. H. Pyrolysis characteristics of Huadian oil shales. *Oil Shale*, 2007, **24**(2), 147–157.
19. Campbell, J. H., Gallegos, G., Gregg, M. Gas evolution during oil shale pyrolysis. 2. Kinetic and stoichiometric analysis. *Fuel*, 1980, **59**(10), 727–732.
20. Nazzal, J. M. Influence of heating rate on the pyrolysis of Jordan oil shale. *J. Anal. Appl. Pyrol*., 2002, **62**(2), 225–238.
21. Campbell, J. H., Koskinas, G. J., Gallegos, G., Gregg, M. Gas evolution during oil shale pyrolysis. 1. Nonisothermal rate measurements. *Fuel*, 1980, **59**(10), 718–726.
22. Campbell, J. H., Koskinas, G. H., Stout, N. D., Coburn, T. T. Oil shale retorting – effects of particle size and heating rate on oil evolution and intraparticle oil degradation. *In Situ* (United States), 1978, **2**(1), 1–47.
23. Han, X. X., Jiang, X. M., Cui, Z. G. Studies of the effect of retorting factors on the yield of shale oil for a new comprehensive utilization technology of oil shale. *Appl. Energ*., 2009, **86**(11), 2381–2385.
24. Johnson, W. F., Walton, D. K., Keller, H. H., Couch, E. J. In situ retorting of oil shale rubble: a model of heat transfer and product formation in oil shale particles. *Colo. School Mines Q*., 1975, **70**(3), 237–272.
25. Al-Ayed, O. S., Al-Harahsheh, A., Khaleel, A. M., Al-Harahsheh, M. Oil shale pyrolysis in fixed-bed retort with different heating rates. *Oil Shale*, 2009, **26**(2), 139–147.
26. Al-Ayed, O. S., Suliman, M. R., Rahman, N. A. Kinetic modeling of liquid generation from oil shale in fixed bed retort. *Appl. Energ*., 2010, **87**(7), 2273–2277.
27. Raley, J. H. Monitoring oil shale retorts by off-gas alkene/alkane ratios. *Fuel*, 1980, **59**(6), 419–424.
28. Burnham, A. K., Ward, R. L. A possible mechanism of alkene/alkane production in oil shale retorting. *ACS Div. Fuel Chem. Preprints*, 1980, **25**, 82–88.
29. Shen, M.-S., Lui, A. P., Shadle, L. J., Zhang, G.-Q., Morris, G. J. Kinetic studies of rapid oil shale pyrolysis. 2. Rapid pyrolysis of oil shales in a laminar-flow entrained reactor. *Fuel*, 1991, **70**(11), 1277–1284.
30. Al-Harahsheh, A., Al-Ayed, O., Al-Harahsheh, M., Abu-El-Halawah, R. Heating rate effect on fractional yield and composition of oil retorted from El-lajjun oil shale. *J. Anal. Appl. Pyrol*., 2010, **89**(2), 239–243.
31. Ahmad, N., Williams, P. T. Influence of particle grain size on the yield and composition of products from the pyrolysis of oil shales. *J. Anal. Appl. Pyrol*., 1998, **46**(1), 31–49.
32. Nazzal, J. M. The influence of grain size on the products yield and shale oil composition from the pyrolysis of Sultani oil shale. *Energ. Convers. Manage*., 2008, **49**(11), 3278–3286.

33. Hurst, H. J., Levy, J. H., Patterson, J. H. Siderite decomposition in retorting atmospheres. *Fuel*, 1993, **72**(6), 885–890.
34. Nazzal, J. M. The presence of polycyclic aromatic hydrocarbons (PAH) in oil obtained at pyrolysis of Jordan oil shale. *Oil Shale*, 2007, **24**(3), 465–475.
35. Williams, P. T., Nazzal, J. M. Polycyclic aromatic compounds in oils derived from the fluidised bed pyrolysis of oil shale. *J. Anal. Appl. Pyrol*., 1995, **35**(2), 181–197.
36. Burnham, A. K. Chemistry of shale oil cracking. In *Oil Shale, Tar Sands, and Related Materials* (Stauffer, H. C., ed.). American Chemical Society Symposium Series, 1981, **163**(Chap. 4), 39–60.
37. Stout, N. D., Koskinas, G. J., Raley, J. H., Santor, S. D., Opila, R. J., Rothman, A. J. Pyrolysis of oil shale: the effects of thermal history on oil yield. *Colo. School Mines Q*., 1976, **71**, 153–172.
38. Sun, Z. L. *Evaluation and Analysis of Crude Oils*. China Petrochemical Press, Beijing, 2005 (in Chinese).
39. Lin, S. X. *Petroleum Refining Engineering* (Third Edition). Petroleum Industry Press, Beijing, 2000 (in Chinese).
40. Williams, P. F. V. Thermogravimetry and decomposition kinetics of British Kimmeridge Clay oil shale. *Fuel*, 1985, **64**(4), 540–545.
41. Wallman, P. H., Tamm, P. W., Spars, B. G. Oil shale retorting kinetics. In *Oil Shale, Tar Sands, and Related Materials* (Stauffer, H. C., ed.). American Chemical Society Symposium Series, 1981, **163**(Chap. 7), 93–113.
42. Trejo, F., Ancheyta, J., Centeno, G., Marroquín, G. Effect of hydrotreating conditions on Maya asphaltenes composition and structural parameters. *Catal. Today*, 2005, **109**(1-4), 178–184.
43. Ancheyta, J., Centeno, G., Trejo, F., Marroquín, G. Changes in asphaltene properties during hydrotreating of heavy crudes. *Energ. Fuel*., 2003, **17**(5), 1233–1238.

Presented by S. Li
Received April 4, 2012